Electronic Supporting Information (ESI)

A Co and Fe bimetallic MOF with enhanced electrocatalytic oxygen evolution performance: exploring the electronic environment modifications upon Fe incorporation †

Varsha Singh,[a] Devesh Kumar Singh,[b] Mamta Yadav,[a] Smita Singh,[a] Vikram Rathour,[a] Ananya Tiwari,[a] and Vellaichamy Ganesan[a]*

a: Department of Chemistry, Institute of Science, Banaras Hindu University, Varanasi-221005, UP, India

b: Kutir Post Graduate College, Chakkey, Jaunpur-222146, UP, India

E-mail: velganesh@yahoo.com and velgan@bhu.ac.in

*Corresponding author

Calculation of turnover frequency (TOF)

The turnover frequency is calculated by measuring the cyclic voltammetry (CV) response in the non-catalytic redox region (in this case, 0.9 to 1.4 V (*vs.* RHE)). Half of the integrated area of the cyclic voltammogram is divided by the scan rate at which the CV is recorded (in this case, 0.02 V s^{-1}) to get the charge.

Charge (Coulombs) = Half of the integrated area of the cyclic voltammogram (V A) /scan rate (V s^{-1})

Number of electrons = Charge/1.602×10^{-19}

The obtained number of electrons was divided by electrons transferred in the redox reaction (in this case, 1 corresponding to Co^{2+} to Co^{3+}) to get the surface concentration (c)

$TOF = (i \times N_A)/A \times F \times n \times c$

where, i = current in A

N_A = Avogadro number (6.023×10^{23})

A = Geometrical area of the electrode (here 0.196 cm^2)

F = Faraday constant (96485 C)

n = number of electrons

c = surface concentration

Table S1: The obtained ratios of Co:Fe comprehended from ICP analysis.

Feed ratio of metal ions (Co:Fe)	Obtained ratio (Co:Fe)
2:1	1.7:1
1:1	1:1.1
1:2	1:2.2

Table S2: XPS peak positions of elements in Co-MOF, Fe-MOF, and 2:1 Co-Fe-MOF.

Materials / Elements	Co-MOF Binding energy / eV	Fe-MOF Binding energy / eV	2:1 Co-Fe-MOF Binding energy / eV
C	284.6 (Adventitious-C) 285.1 (C-C) 285.6 (C-N) 286.2 (C=N-C) 286.9 (C-O) 288.8 (O-C=O)	284.6 (Adventitious-C) 285.0 (C-C) 285.6 (C-N) 286.2 (C=N-C) 287.0 (C-O) 288.6 (O-C=O)	284.6 (Adventitious-C) 285.2 (C-C) 286.1 (C-N) 286.8 (C=N-C) 286.9 (C-O) 288.5 (O-C=O)
Co	783.1 (Co^{2+}) 788.4 (Sat.) 798.7 (Co^{2+}) 804.8 (Sat.)	-	780.7 (Co^{3+}) 796.3 (Co^{3+}) 786.6 (Sat.) 782.4 (Co^{2+}) 797.7 (Co^{2+}) 803.3 (Sat.)
Fe	-	713.7 (Fe^{3+}) 719.2 (Sat.) 727.1 (Fe^{3+})	713.4 (Fe^{3+}) 726.1 (Fe^{3+}) 718.4 (Sat.) 711.0 (Fe^{2+}) 724.1 (Fe^{2+})
N	399.5 (M-N) 400.4 (Pyridinic-N) 407.3 (Nitrate-N)	399.4 (M-N) 400.3 (Pyridinic-N) 407.1 (Nitrate-N)	399.4 (M-N) 400.3 (Pyridinic-N) 406.7 (Nitrate-N)
O	531.1 (M-O) 532.9 (O-C=O) 533.0 (Adsorbed H_2O)	530.2 (M-O) 531.4 (O-C=O) 532.6 (Adsorbed H_2O)	530.0 (M-O) 531.5 (O-C=O) 532.6 (Adsorbed H_2O)

Table S3: Mass activity values ($Ag^{-1}cm^{-2}$) of MOFs at various potentials.

S. No.	MOFs	Mass activity values at different applied potentials (V, *vs.* RHE)			
		1.54	1.59	1.64	1.69
1.	2:1 Co-Fe-MOF	173.89	483.46	879.78	1260.29
2.	1:1 Co-Fe-MOF	76.47	257.47	483.46	815.44
3.	1:2 Co-Fe-MOF	61.03	207.78	379.78	627.57
4.	Co-MOF	16.91	27.94	113.97	258.08

Table S4: TOF values (s^{-1}) of MOFs at various overpotentials.

S. No.	MOFs	TOF values at different overpotentials		
		320 mV	370 mV	420 mV
1.	2:1 Co-Fe-MOF	8.48	26.83	48.36
2.	1:1 Co-Fe-MOF	6.05	19.05	41.16
3.	1:2 Co-Fe-MOF	4.36	17.37	40.95
4.	Co-MOF	0.53	4.26	20.27

Table S5: Evaluation of OER performances of various bimetallic MOFs with present work.

S. No.	MOFs	Substrate	Overpotential (η, mV) at 10 mA. cm^{-2}	Tafel slope (mV/ dec)	References
1.	Ni-BTC	Carbon paper	346	64	[66]
2.	Co-Fe-BDC	GCE	295	34.8	[28]
3.	Co-Fe-IDA	GCE	265	44	[29]
4.	$Co_{0.6}Fe_{0.4}$-MOF74 (DHTA)	GCE	280	56	[67]
5.	2:1 Co-Fe-MOF	GCE	310	45	This work
6.	Ni-Co-BTC	GCE	330	32	[14]
7.	FeNi@CNF	GCE	356	62.6	[20]
8.	Co-Fe-BDC	GCE	238	52	[30]
9.	$[Ni_2(BBTZ)(H_2O)_4]V_4O_{12}\cdot 2H_2O$	Carbon cloth	353	77.8	[68]
10.	$Co_{0.75}Fe_{0.25}$-Pyrazine	GCE	239	42	[69]

BTC: (1,3,5-benzene tricarboxylate), BDC: (1,4-benzene dicarboxylate), (3) IDA: (4,5 imidazole dicarboxylic acid), (4) DHTA: (2,5-dihydroxyterepthalic acid), (7) CNF: complex nanoflower (9) BBTZ: 1,4-bis-(1,2,4-triazol-1-ylmethyl)benzene

Figure S1: Digital photographs of MOFs showing the color variations.

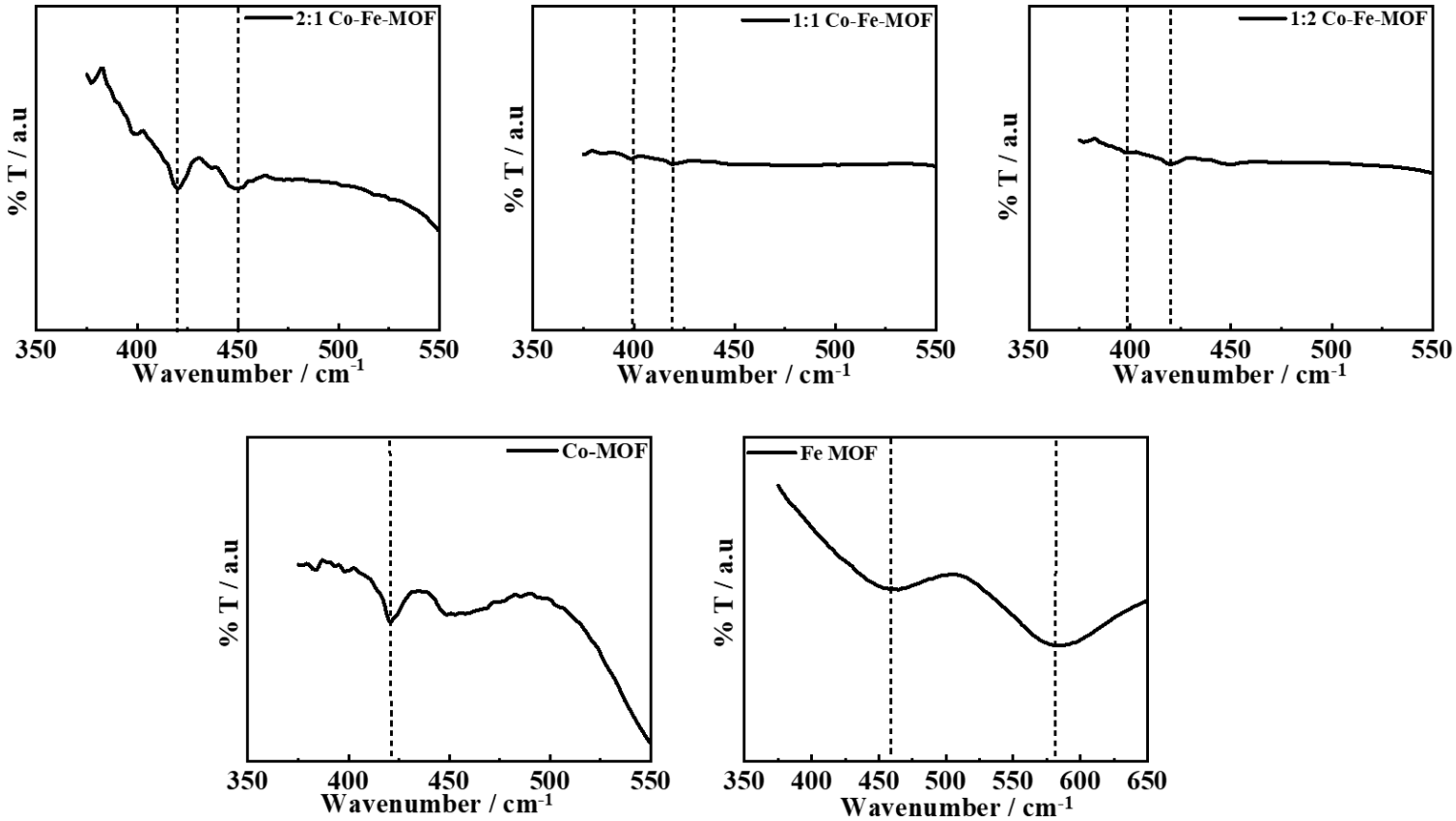

Figure S2: FT-IR spectra showing the presence of M-O and M-N bonds in the MOFs.

.

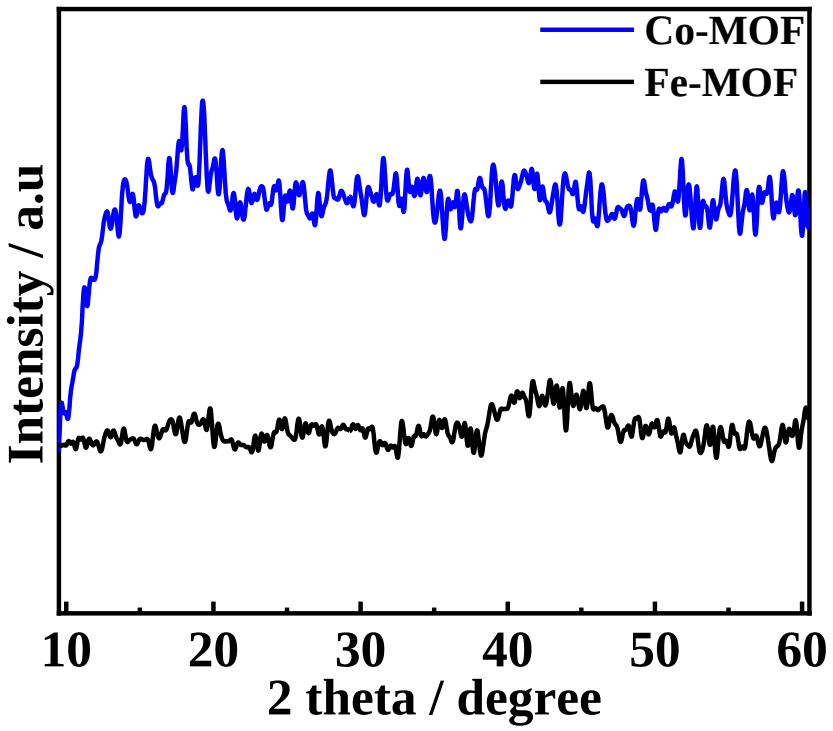

Figure S3: Powder XRD patterns of Co-MOF and Fe-MOF.

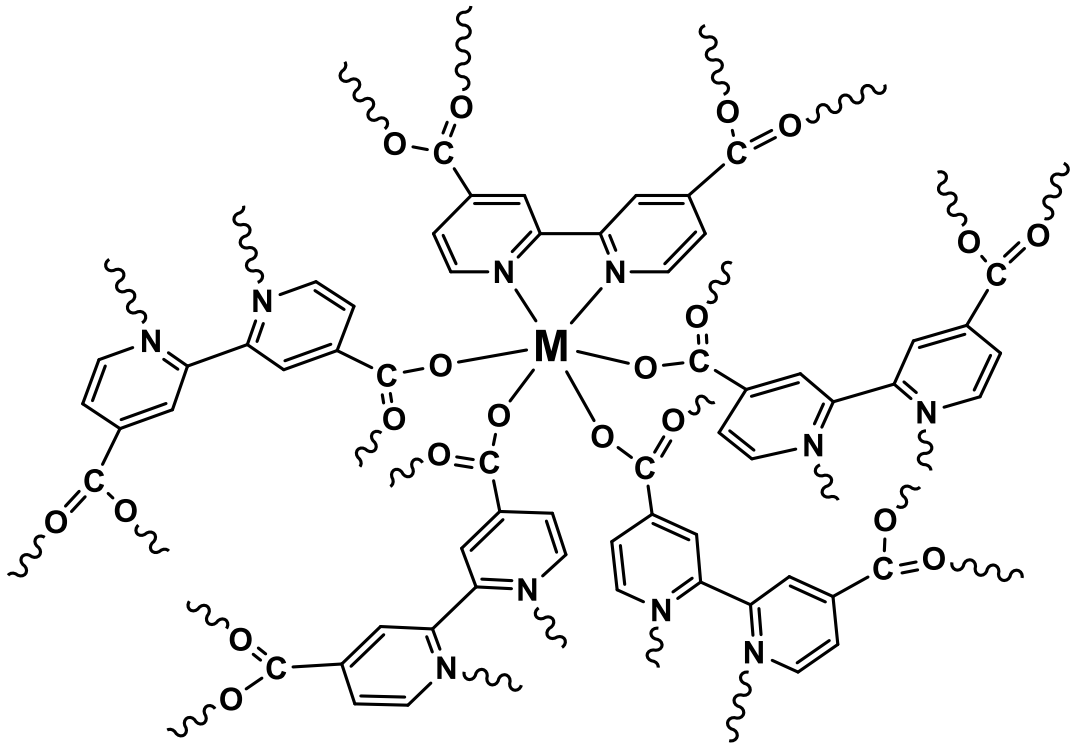

M = Co or Fe

Figure S4: Possible structure of the MOF

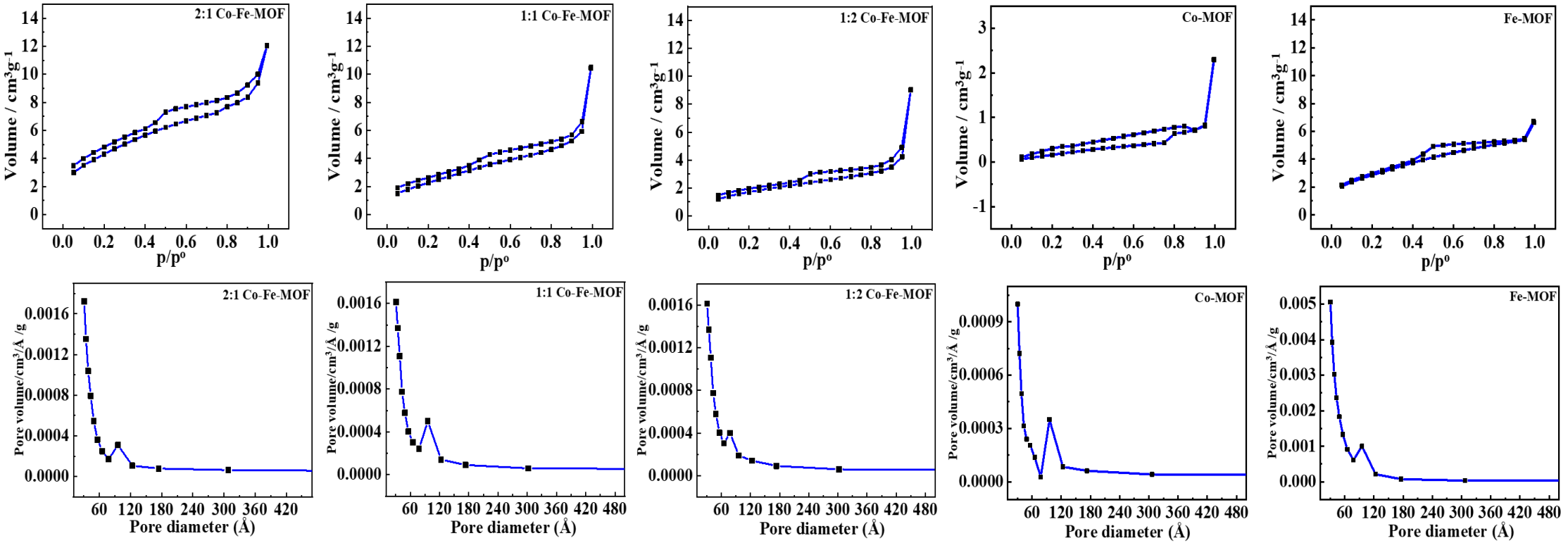

Figure S5: BET surface area and pore size distribution curve of MOFs.

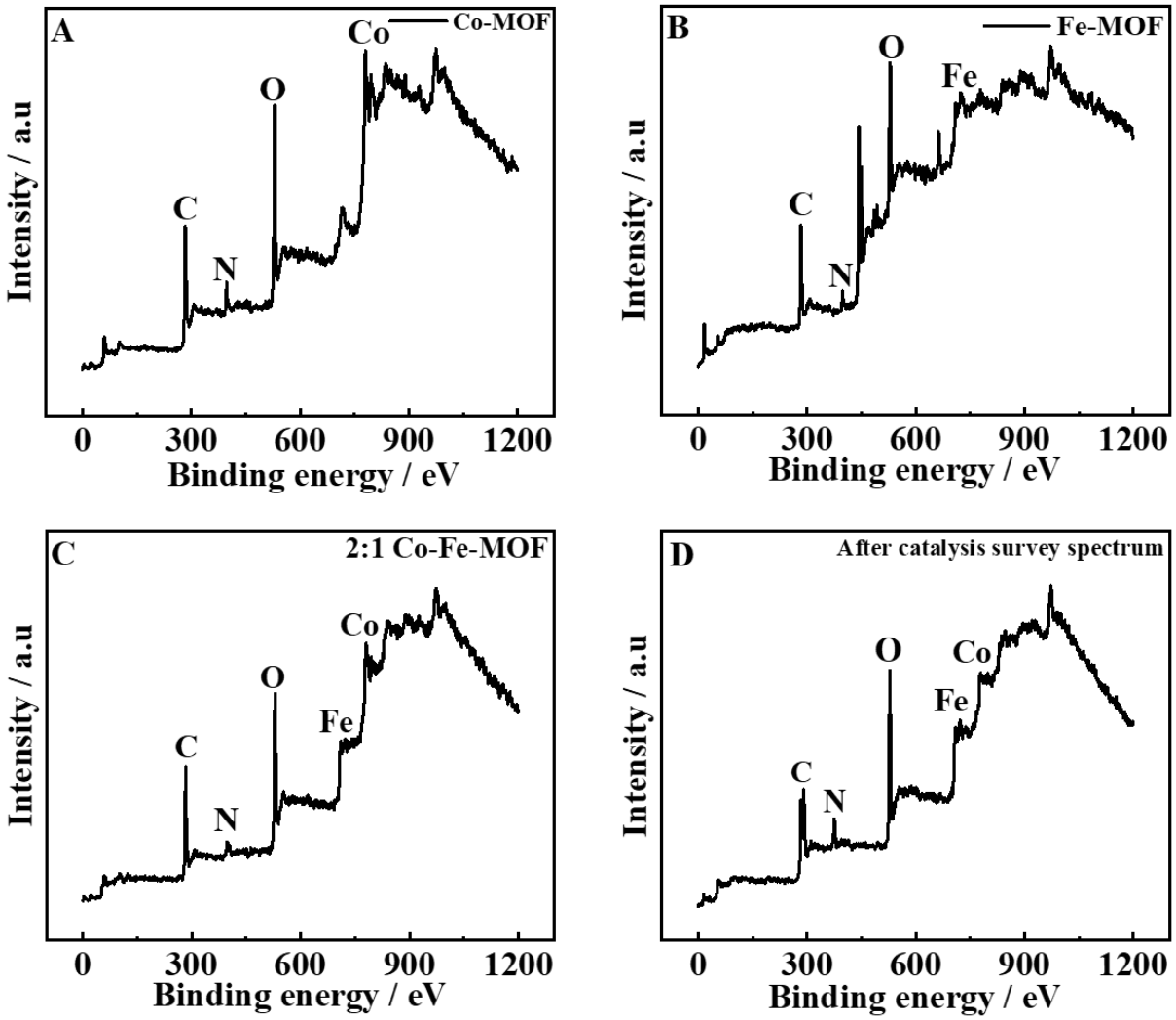

Figure S6: XPS survey spectra of Co-MOF (A), Fe-MOF (B), 2:1 Co-Fe-MOF (C), and after the OER catalysis 2:1 Co-Fe-MOF (D).

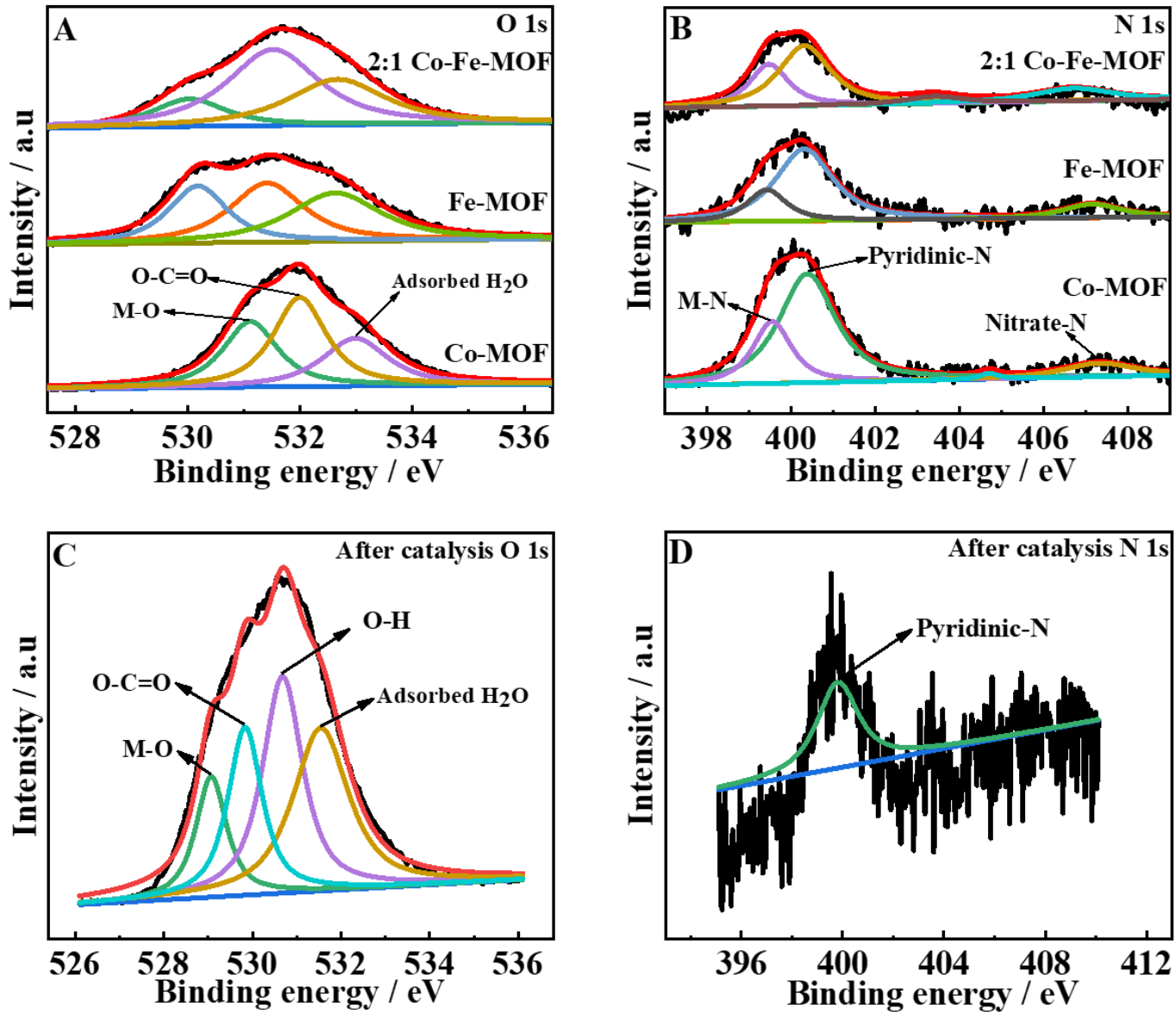

Figure S7: O 1s (A) and N 1s (B) XPS spectra of Co-MOF, Fe-MOF, 2:1 Co-Fe-MOF and after catalysis XPS spectra of O 1s (C) and N 1s (D) of 2:1 Co-Fe-MOF.

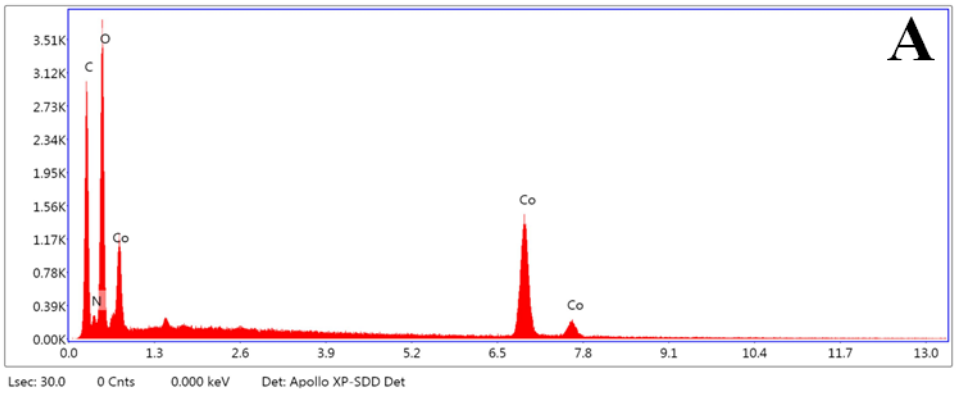

Element	Weight %	Atomic %
C K	33.4	45.6
N K	9.3	10.9
O K	37.0	37.9
CoK	20.3	5.6

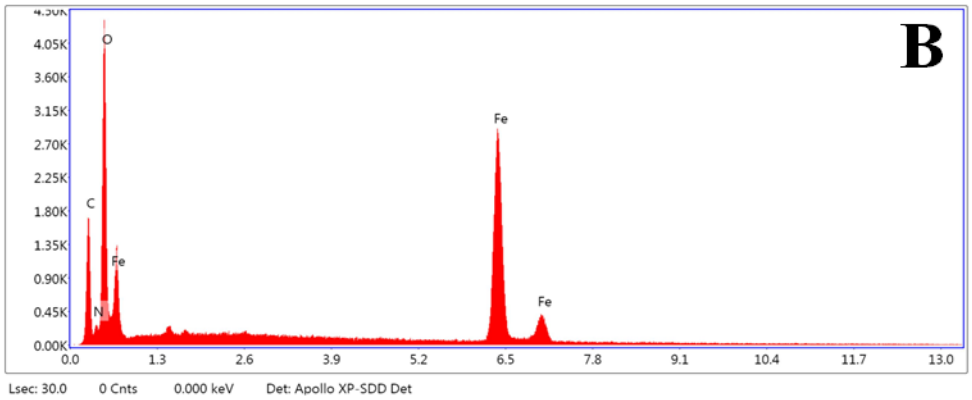

Element	Weight %	Atomic %
C K	23.7	37.6
N K	7.0	9.5
O K	34.4	41.0
FeK	35.0	12.0

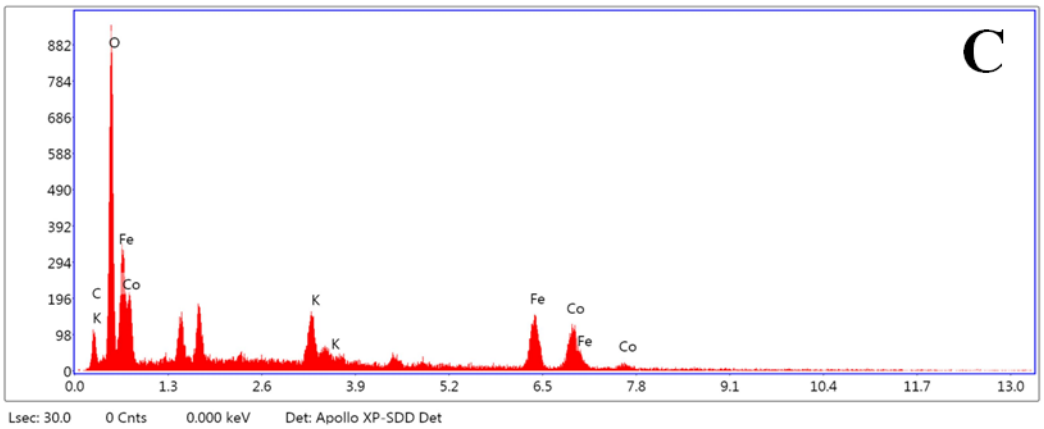

Element	Weight %	Atomic %
C K	25.7	34.5
N K	8.3	9.6
O K	51.2	51.7
K K	0.1	0.0
FeK	5.0	1.5
CoK	9.7	2.7

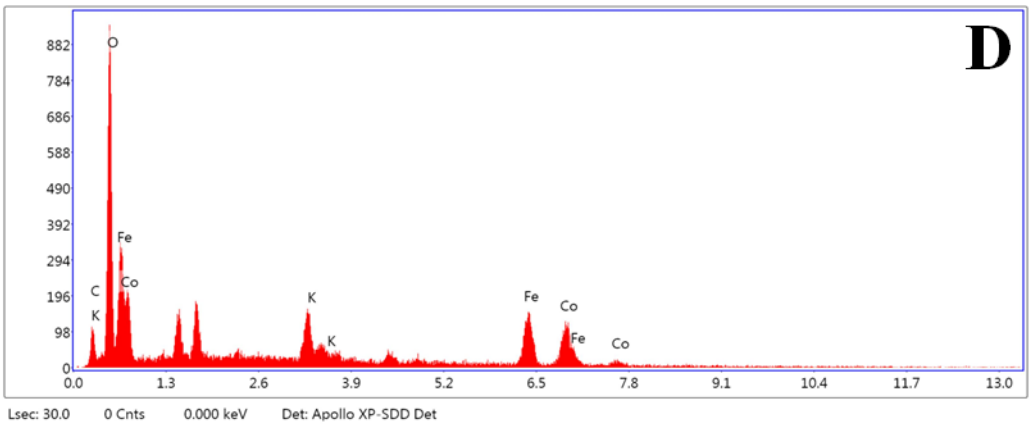

Element	Weight %	Atomic %
C K	21.6	25.9
O K	51.5	64.0
K K	5.1	2.6
FeK	7.2	2.6
CoK	14.7	5.0

Fig. S8: EDX spectra and elemental composition analyses of (A) Co-MOF, (B) Fe-MOF, (C) 2:1 Co-Fe-MOF, and (D) post-catalysis 2:1 Co-Fe MOF

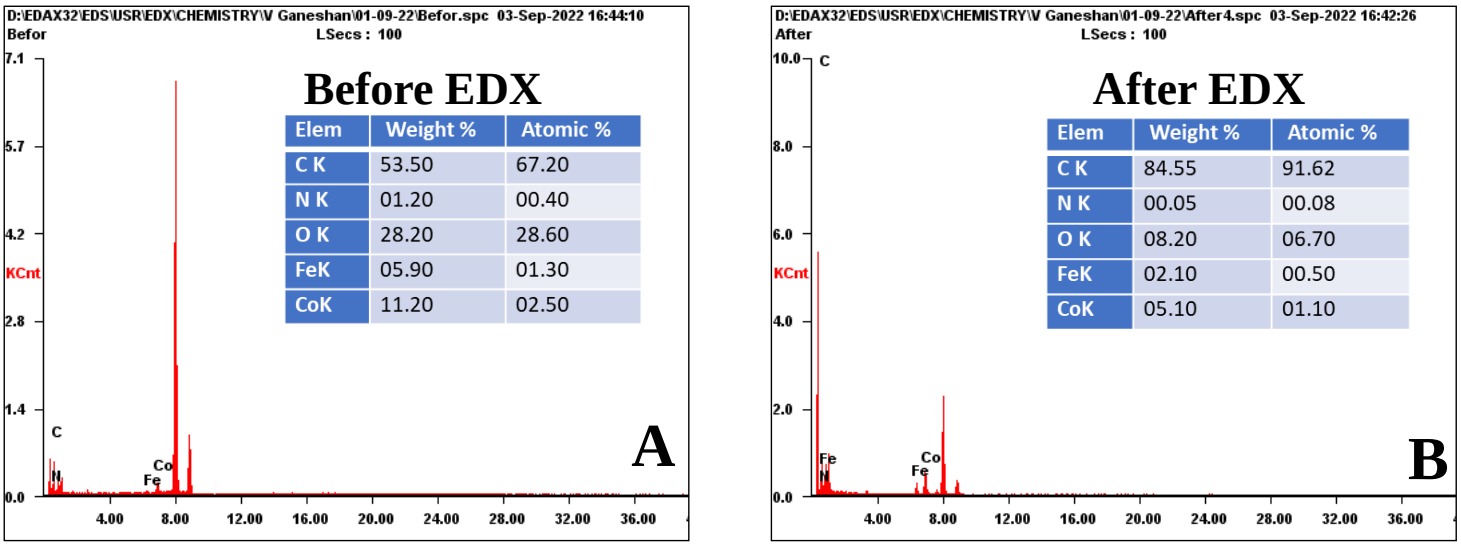

Figure S9: EDX spectra of 2:1 Co-Fe-MOF before (A) and after (B) OER catalysis.

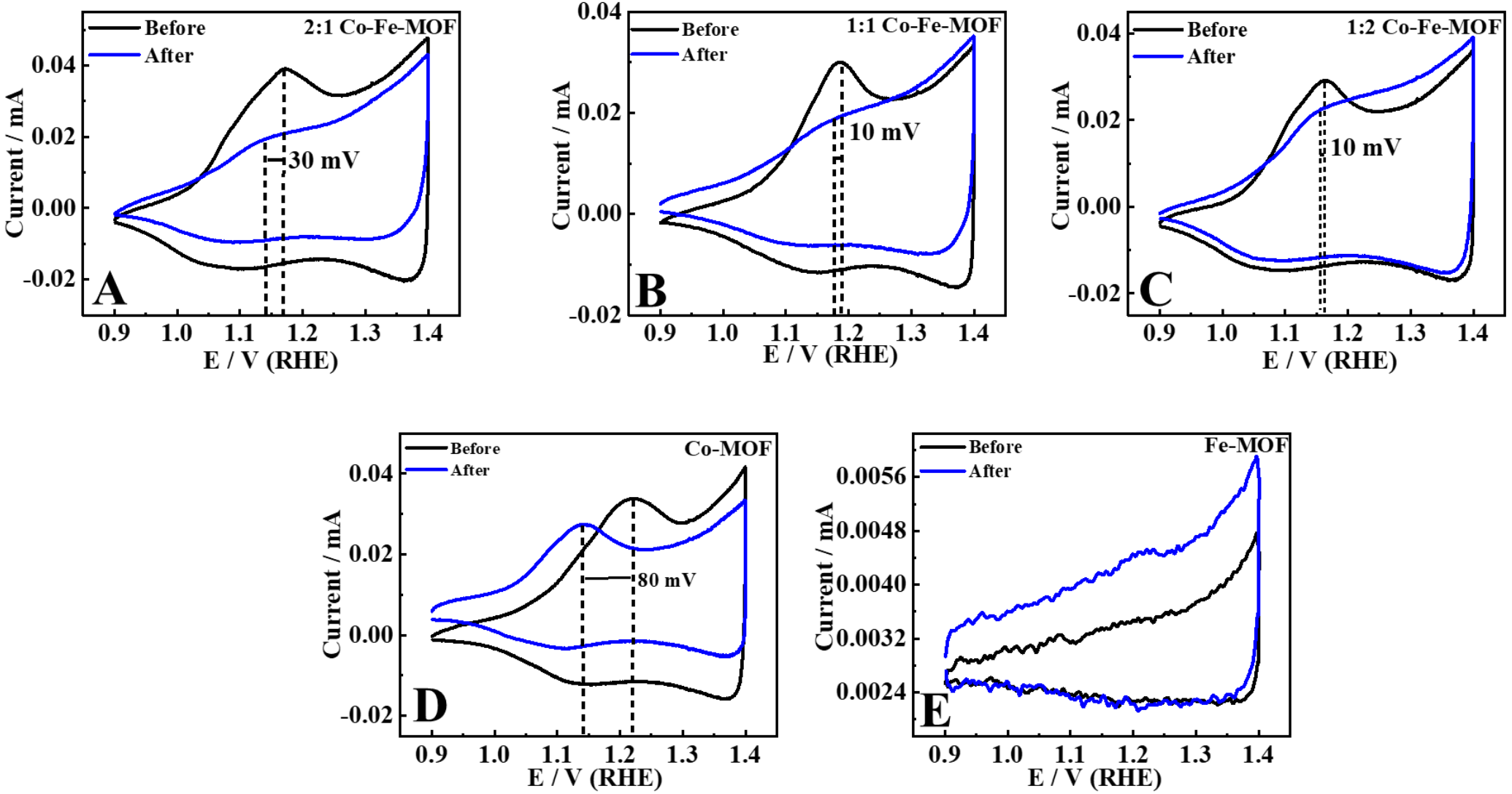

Figure S10: CV responses of MOFs before and after 30 consecutive CV cycles.

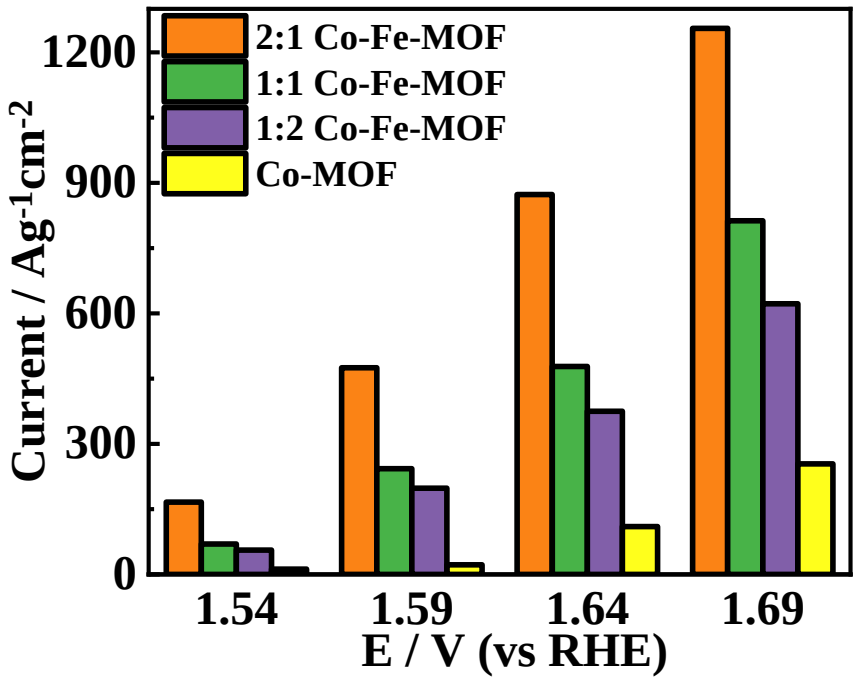

Figure S11: Mass activity plot of MOFs at different potentials.

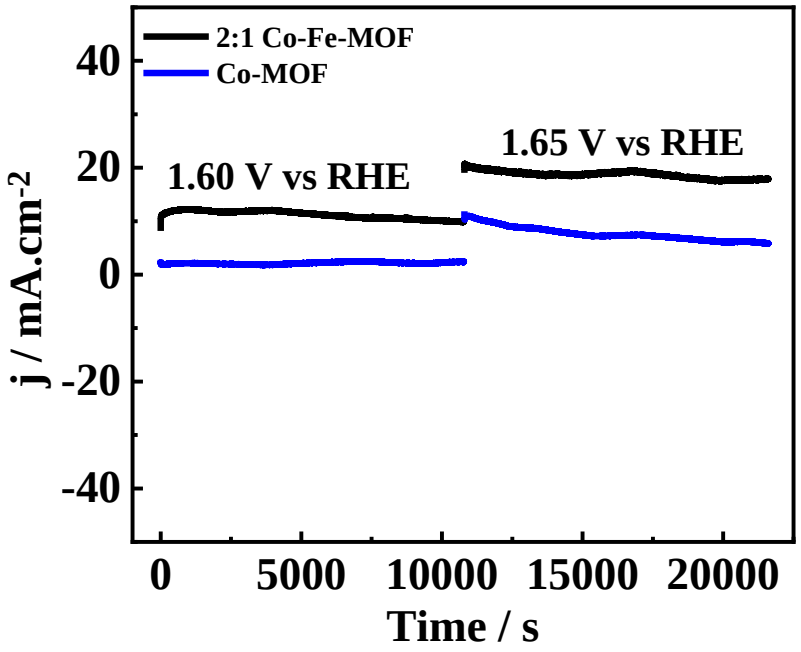

Figure S12: Stability test responses by amperometry 2:1 Co-Fe-MOF and Co-MOF at 1.60 V and 1.65 V *vs* RHE for three hours each.

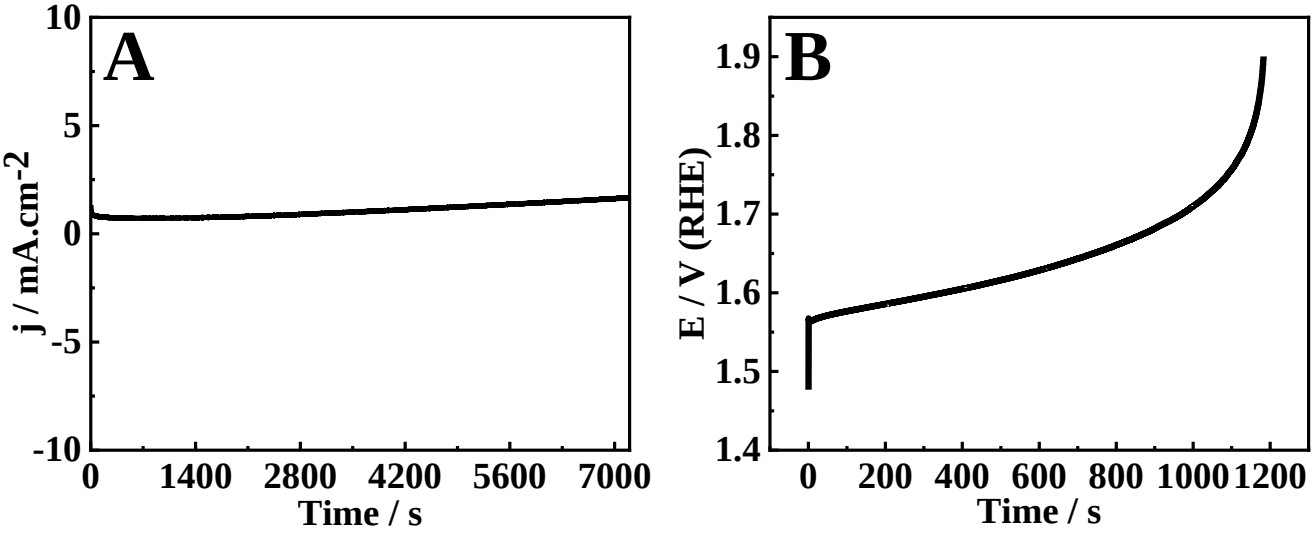

Figure S13: Stability test responses by amperometry (A) and chronopotentiometry (B) of GC_{RDE}/RuO_2.

References

S1:S. Anantharaj, P. E. Karthik and S. Kundu, Petal-like hierarchical array of ultrathin $Ni(OH)_2$ nanosheets decorated with $Ni(OH)_2$ nanoburls: A highly efficient OER electrocatalyst, *Catal. Sci. Technol.*, 2017, **7**, 882–893.